Indian Geotech J (July–September 2012) 42(3):150–160
DOI 10.1007/s40098-012-0018-2

ORIGINAL PAPER

How Well Do We Understand Earthquake Induced Liquefaction?

Gopal S. P. Madabhushi · Stuart K. Haigh

Received: 25 June 2012 / Accepted: 4 July 2012 / Published online: 15 July 2012

Abstract Soil liquefaction following large earthquakes is a major contributor to damage to infrastructure and economic loss, as borne out by the earthquakes in Japan and New Zealand in 2011. While extensive research has been conducted on soil liquefaction and our understanding of liquefaction has been advancing, several uncertainties remain. In this paper the basic premise that liquefaction is an 'undrained' event will be challenged. Evidence will be offered based on dynamic centrifuge tests to show that rapid settlements occur both in level ground and for shallow foundations. It will also be shown that the definition of liquefaction based on excess pore pressure generation and the subsequent classification of sites as liquefiable and non-liquefiable is not satisfactory, as centrifuge test data shows that both loose and dense sand sites produce significant excess pore pressure. Experimental evidence will be presented that shows that the permeability of sands increases rapidly at very low effective stresses to allow for rapid drainage to take place from liquefied soil. Based on these observations a micro-mechanical view of soil liquefaction that brings together the Critical State view of soil liquefaction and the importance of dynamic loading will be presented.

Keywords Critical state · Earthquakes · Liquefaction · Permeability · Undrained

Introduction

Earthquake-induced liquefaction has resulted in severe damage to many civil engineering structures. This is true for historic earthquakes such as the 1964 Niigata earthquake in Japan and the Alaskan earthquake in the USA as well as for more recent earthquakes such as the earthquakes in Turkey and Taiwan in 1999, the 2001 Bhuj earthquake in India and the 2011 earthquake in New Zealand.

Liquefaction of ground can result in several different types of damage. An example of liquefaction induced damage at the Lyttleton Port near Christchurch is shown in Fig. 1. In this figure the differential settlement of a wharf causing rotation of a historical light house can be seen. Another example of the damage to a footbridge can be seen in Fig. 2. The inward movement of the river banks following liquefaction caused this footbridge to suffer a torsional buckling failure. Soil liquefaction is known to cause settlement and rotation of buildings. An example of the settlement and rotation suffered by a single-storied residential building is shown in Fig. 3. Although all these failures are different, the underlying cause of their predicament is soil liquefaction. Madabhushi and Haigh [22] studied bridge failures due to liquefaction in the Bhuj earthquake in India and suggested that the super-structure stiffness has played an important role in the mode of liquefaction-induced failures.

Research into soil liquefaction started soon after the 1964 earthquakes in Japan and Alaska. The last two decades have seen a great advancement of both the scientific understanding of liquefaction phenomena and of modelling liquefaction using numerical and centrifuge modelling, particularly with the establishment of the George E Brown Network of Earthquake Engineering Simulation (NEES) in the USA and similarly the UK-NEES network. The failure mechanisms of buildings, piles, retaining walls and bridge foundations have been widely investigated.

Despite these advancements, there are several aspects of liquefaction that remain unclear. The definition of liquefaction

G. S. P. Madabhushi (✉) · S. K. Haigh
Department of Engineering, University of Cambridge, Cambridge, UK
e-mail: mspg1@cam.ac.uk

Fig. 1 Damage to a historic light house at Lyttleton port

Fig. 2 Torsional buckling failure of a footbridge due to liquefaction-induced movement of the river banks

may be considered as a specific example. Soil liquefaction may be defined, using Terazaghi's effective stress principle, as the state of saturated soils when the pore pressure matches the total stress, thereby reducing the effective stress to zero.

$$\sigma'_v = \sigma_v - \left(u_{\text{hyd}} + u_{\text{excess}}\right) \quad (1)$$

where u_{hyd} and u_{excess} are hydrostatic and excess pore pressures, respectively.

The total stress σ_v, is usually considered to be the geostatic vertical stress. This definition is appropriate for level

Fig. 3 Settlement and rigid body rotation of a house following soil liquefaction

ground with no buildings or other structures. When considering a soil element below a building, the total stress in the soil is affected by the bearing pressure exerted by the building and therefore a higher excess pore pressure may be required to liquefy the soil. This is, however, difficult to determine, as the stress distribution due to the structure changes with the onset of liquefaction. Coelho et al. [8] show that the stress distribution below a shallow foundation narrows down with liquefaction, forming a column of highly stressed soil underneath the foundation that remains non-liquefied while the free field soil fully liquefies. Similar observations were also made by Ghosh and Madabhushi [11], who investigated excess pore pressure generation underneath a heavy foundation for a nuclear reactor building. Underneath a building, the vertical effective stress therefore changes with the evolution of excess pore pressures generated by earthquake loading from two viewpoints. Firstly, using Eq. 1, the effective stress decreases as excess pore pressures increase. Secondly, the change in stress distribution below the building causes the total and hence effective stresses to change. Thus the definition of liquefaction, given earlier, needs to be updated. It must be understood that the value of effective stress in Eq. 1 is not the free field effective stress or the initial effective stress. It must be the effective stress at any given point and at any given time, where the excess pore pressure is known. It must also be pointed out that in this paper the subtle differences between 'initial liquefaction' and 'flow liquefaction' [18] have not been considered.

Historical Evolution of Liquefaction Concepts

Casagrande [5] proposed the existence of a 'critical void ratio' for sands, based on his load-controlled drained shear

box tests. He envisaged that when a natural soil deposit has a void ratio equals to or greater than this 'critical void ratio', it is susceptible to liquefaction failure. Casagrande [6] described the observation of liquefaction in undrained cyclic loading of saturated sands in triaxial tests as the point at which there is a substantial loss of shear strength when the sand is subjected to continuous shear strains. Further, he described the point at which the pore pressure in the sample equals the cell pressure in a cyclic triaxial test on a dense sand sample as 'cyclic mobility'.

Castro [7] associated liquefaction with a sudden loss of shear strength resulting in a catastrophic failure. In laboratory tests, he observed that a sample of sand subjected to cyclic or monotonic loading exhibited liquefaction failure only if the driving stresses were larger than the undrained shear strength of the sample. Following earthquake loading and the subsequent generation of excess pore pressures in saturated sands, the driving shear stresses below a building can be greater than the undrained shear strength. Castro considered the steady state deformations that occur in the presence of elevated pore pressures following earthquake loading as liquefaction failure. This was thought to be justified, as many dams such as the upper and lower San Fernando dams were known to have failed after the end of earthquake loading [9]. Dixon and Burke observed that there was a possibility of liquefaction occurring at great depths below these dams contrary to the opinion of Casagrande [6].

Seed and Lee [31] listed the factors that may affect excess pore pressure generation in sands as being void ratio, number of cycles of applied shear stress, effective confining pressure and the magnitude of applied shear stress and shear strains. Seed et al. [32] carried out dynamic analysis of the Sheffield dam and attributed its failure to the generation of excess pore pressures that equalled the total stress, leading to a condition of 'zero' effective stress. This condition, presented in Eq. 1 earlier, was associated by Seed to 'liquefaction failure'. Further, his insistence on the importance of consideration of excess pore pressure generation in cyclic loading came true following the 1971 San Fernando earthquake that caused failure of the upper and lower San Fernando dams, [9].

Roscoe et al. [27] and Schofield and Wroth [30] established the Critical State soil mechanics framework based on the postulation that a soil element that has reached a Critical State will continuously deform without further changes in stress or volume. This state can be depicted as a single line in q–p′–v space. Schofield [28, 29] and later Muhunthan and Schofield [25] applied the Critical State framework to soil liquefaction. Consider the stress state of a soil element on the loose or 'wet' side of the Critical State. When this soil element is subjected to cyclic shear stresses under undrained conditions, the propensity to suffer volumetric contraction is manifested as an increase in excess pore water pressures. This causes the effective confining stress to reduce, as shown in Fig. 4. Eventually, the stress path will cross the tensile rupture or fracture surface resulting in a disaggregation of the continuum into a clastic body with unstressed grains free to slide apart. This results in the massive loss of strength seen during liquefaction.

Luong [19] suggested using the characteristic state theory to understand the behaviour of sand subjected to cyclic loading. He proposed that above a characteristic stress ratio, in the sur-characteristic region identified in Fig. 5, dilatant behaviour is exhibited by the sand sample. Below the characteristic state line, in the sub-characteristic region, contractile behaviour will be observed. Luong and Sidaner [20] found experimentally, based on cyclic triaxial tests, that the characteristic state line can be expressed as a single line in q–p′ space on the compression side. For the extension side, a similar line with a shallower slope was found.

Quite independent to the work of Luong, Ishihara et al. [14] conducted a series of cyclic triaxial tests on saturated Toyura sand and observed that whenever the stress ratio exceeded a specific value, large pore pressures developed on unloading. The stress ratio was again expressed as a single line in q–p′ space, but Ishihara et al. [14] and Ishihara [17] called it a phase transformation line. Thus the phase transformation line demarcates the contractile and dilatant behaviour of sands in q–p′ space.

The phase transformation line and the characteristic state line concepts are trying to capture the same behaviour of saturated sands subjected to cyclic loading. Both identify a unique line that demarcates the contractile and dilatant behaviour of sand. It could also be argued that these two concepts are very similar to the Critical State framework for liquefaction proposed by Schofield [28]. The main difference is that the Critical State theory states that once

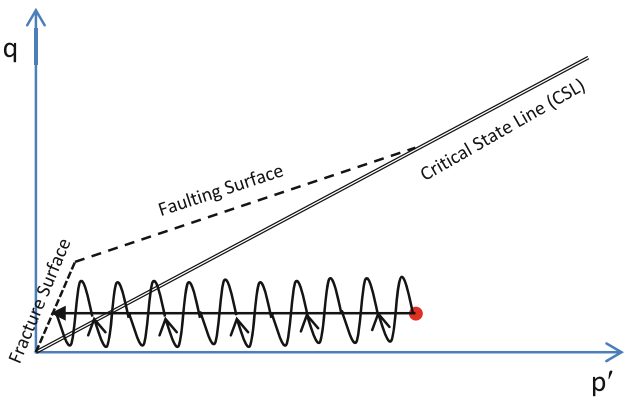

Fig. 4 Critical State framework for soil liquefaction (after Muhunthan and Schofield [25])

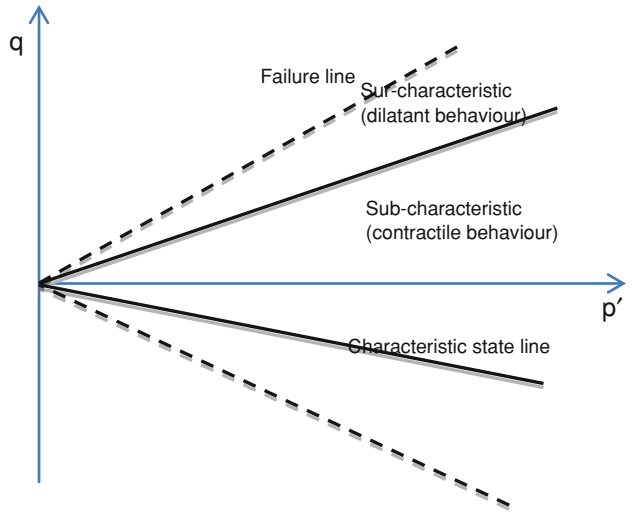

Fig. 5 Characteristic states for sand (after Luong [19])

the stress path of a soil element reaches CSL, it has to stay on this line. The characteristic state theory suggests that the behaviour of the soil changes from contractile to dilatant on crossing the characteristic state (or phase transformation) line before the stress path reaches the failure line. In other words, the slope of the characteristic state line is gentler than that of the Critical State line.

Overall there has been a steady increase in the understanding of liquefaction phenomena over the past five decades. Cyclic triaxial tests and advanced centrifuge tests on liquefiable soils have improved our understanding of liquefaction phenomena. The theoretical frameworks for liquefaction described above are able to capture the complex cyclic behaviour of saturated sands well. In this paper, however, some fundamental questions will be raised with respect to the definitions used to describe liquefaction phenomena, the methods used to assess the liquefaction potential of a site and the need to describe post-liquefaction behaviour of structures founded on liquefiable soils. The last point is particularly important given the need to estimate the ground deformations close to structures as demanded by 'performance based design'.

Methodologies Used for Liquefaction Assessment of a Site

Seed and Idriss [33] and Seed [34] were the first researchers to link the Standard Penetration Test (SPT) data for a given site to its liquefaction potential. The original curves are binary in nature i.e. they demarcate liquefiable and non-liquefiable sites. This concept became extremely popular and is widely used in North America and worldwide. Many changes have been proposed to the original charts over the years, resulting in more recent examples such as those proposed by Idriss and Boulanger [13]. In Europe, Eurocode 8 proposes a similar curve, shown in Fig. 6, to be used for liquefaction assessment. The shear stress generated by the earthquake loading is normalised by the initial vertical stress and plotted on the *y*-axis, while the corrected SPT values are plotted on *x*-axis. The three curves in the figure, each for a different percentage of fines, demarcate liquefiable from non-liquefiable sites. Further, many researchers proposed other site investigation data to be used for liquefaction assessment of a site. For example, Robertson and Wride [26] correlated CPT data from sites with SPT data and hence developed a chart to assess liquefaction potential of sites. Similarly shear wave velocity (V_s) profiles measured are linked by Andrus and Stokoe [1] to the liquefaction potential of sites.

While the use of liquefaction assessment charts is prevalent worldwide, they have many disadvantages. For example, the SPT value of a site may indicate that it falls quite close to, but below, the liquefaction line. While the chart suggests that the site will not liquefy, significant excess pore pressures may still be generated causing damage to structures located on such sites [23]. Such binary charts are therefore of limited use as they do not indicate how much excess pore pressures will be generated in a given earthquake or how much volumetric strain will the site suffer, exhibited as ground settlement. Tokimatsu and Seed [35] addressed some of these issues by relating

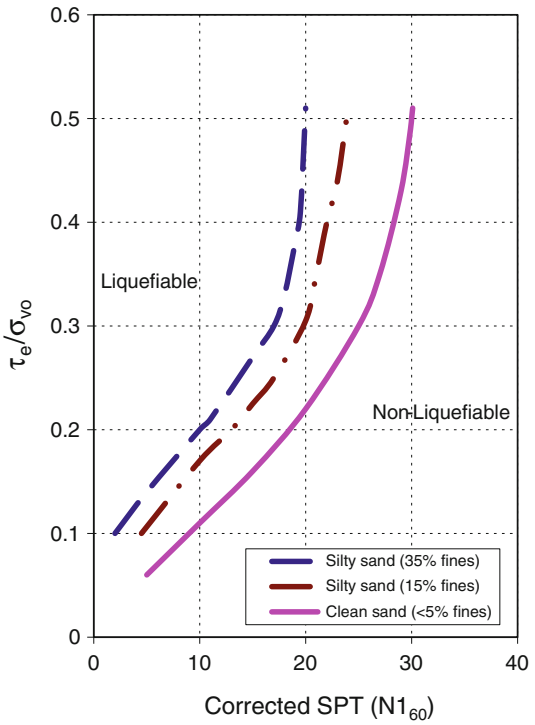

Fig. 6 Liquefaction potential chart, re-plotted from Madabhushi et al. [24]

the volumetric strains to the SPT values based on field observations and triaxial testing.

In this paper it will be demonstrated that saturated sand deposits that were made deliberately loose (RD $\sim$ 50 %) and dense (RD $\sim$ 80 %) both produce significant excess pore water pressures in dynamic centrifuge experiments. If it is accepted that SPT values from a site will be proportional to the relative density of the soil strata, then, based on these experimental results, it can be argued that low and high SPT valued sites can both result in generation of large excess pore pressures. This brings into question the assessment of sites as liquefiable and non-liquefiable, using charts such as the one presented in Fig. 6, particularly if the definition of liquefaction is based on the concept defined by Eq. 1.

Is Liquefaction an Undrained Event?

Liquefaction is traditionally considered to be an undrained event, as the earthquake loading is rapid with the frequency of loading being 1–5 Hz. Thus the tendency to suffer contractile volumetric strains due to cyclic shear strains is manifested as a generation of excess pore pressures in the soil. Many researchers (e.g. [14], [20]), therefore started looking at the liquefaction behaviour of sands using undrained cyclic triaxial tests. Ishihara and Li [15] and Ishihara [16] reported torsional shear tests on loose and dense sand samples as shown in Fig. 7. In this figure it can be seen that both loose and dense sands have similar behaviour in terms of excess pore pressure generation and a consequent drop in effective confining pressure. Application of shear stress once the soil passes the phase transformation line causes the dense sand to be strongly dilative while the loose sand is mildly dilative and needs more strain to display this behaviour. Similar observations can be made based on cyclic triaxial data reported by Luong and Sidaner [20] on Fontainbleau sand, as shown in Fig. 8. Arulmoli et al. [2] tested Nevada sand extensively as part of the VELACS project. They demonstrated that application of static shear to a triaxial sample, before the application of the cyclic strains results in asymmetric stress–strain loops, as shown in Fig. 9. This aspect will be considered later when dealing with liquefaction under shallow foundations. All these tests demonstrate the understanding of soil liquefaction that was developed using undrained triaxial testing.

The development of the liquefaction assessment charts referred to in Fig. 6 earlier and the estimation of volumetric strains were also driven by experimental data from undrained cyclic triaxial tests. Further, many numerical analyses of liquefaction problems based on the finite element method also assume undrained conditions e.g. Finn et al. [10], Beaty and Byrne [3]. Constitutive models for these FE analysis, such as the P-Z mark III model [36], are often calibrated against cyclic triaxial test data such as that shown in Figs. 7, 8 and 9.

Following Fig. 4, however, the stress state of the soil nearing zero effective confining pressure (i.e. liquefaction) takes it towards the fracture line. Once the soil reaches this line it must develop cracks and fissures and allow gaps to open between the soil grains. This would essentially change the soil structure and should result in an increased permeability of the soil with the cracks and fissures conducting the pore water quickly to the soil surface. This argument leads to the conclusion that liquefaction may not be a wholly undrained event. In the undrained cyclic triaxial tests referred to earlier, changes in permeability may not be captured. By definition the undrained tests will not allow for pore fluid drainage while in the field the soil permeability may change due to cracks and fissures opening and allowing for rapid fluid migration. Thus the hypothesis that 'soil liquefaction may not be an undrained event' will have some important implications to the perception of soil liquefaction events and their modelling.

Liquefaction of Level Sand Beds

In 2004 dynamic centrifuge tests were carried out on loose and dense sand layers by Coelho et al. [8]. These were horizontal, fully saturated sand beds tested at $50\times g$'s with prototype dimensions of 33.6 m long and 18.2 m deep. The soil used was uniformly graded Fraction E sand (Leighton Buzzard 100/170). This silica sand was extensively used in many research projects at Cambridge and its properties are well established. While the models were heavily instrumented as reported by Coelho et al. in this paper only three instruments will be considered as shown in Fig. 10. These will be the base accelerometer (ACC) that records the input acceleration, a pore pressure transducer (PPT) at a depth of 14.6 m (292 mm at model scale) that records excess pore pressures and a surface LVDT that measures soil settlement. Again only two tests with relative density of soil model of 50 % (loose) and 80 % (dense) will be considered here, although more tests were carried out at intermediate relative densities, Coelho et al. [8].

In Figs. 11 and 12, the results from dynamic centrifuge tests on soil deposits with relative densities of 50 and 80 % are presented. Both models were subjected to very similar earthquake loading with a peak horizontal acceleration of $8\times g$ with nominally 10 cycles. This peak acceleration of $8\times g$ is equivalent to $0.16\times g$ of peak acceleration applied at the bedrock level at prototype scale.

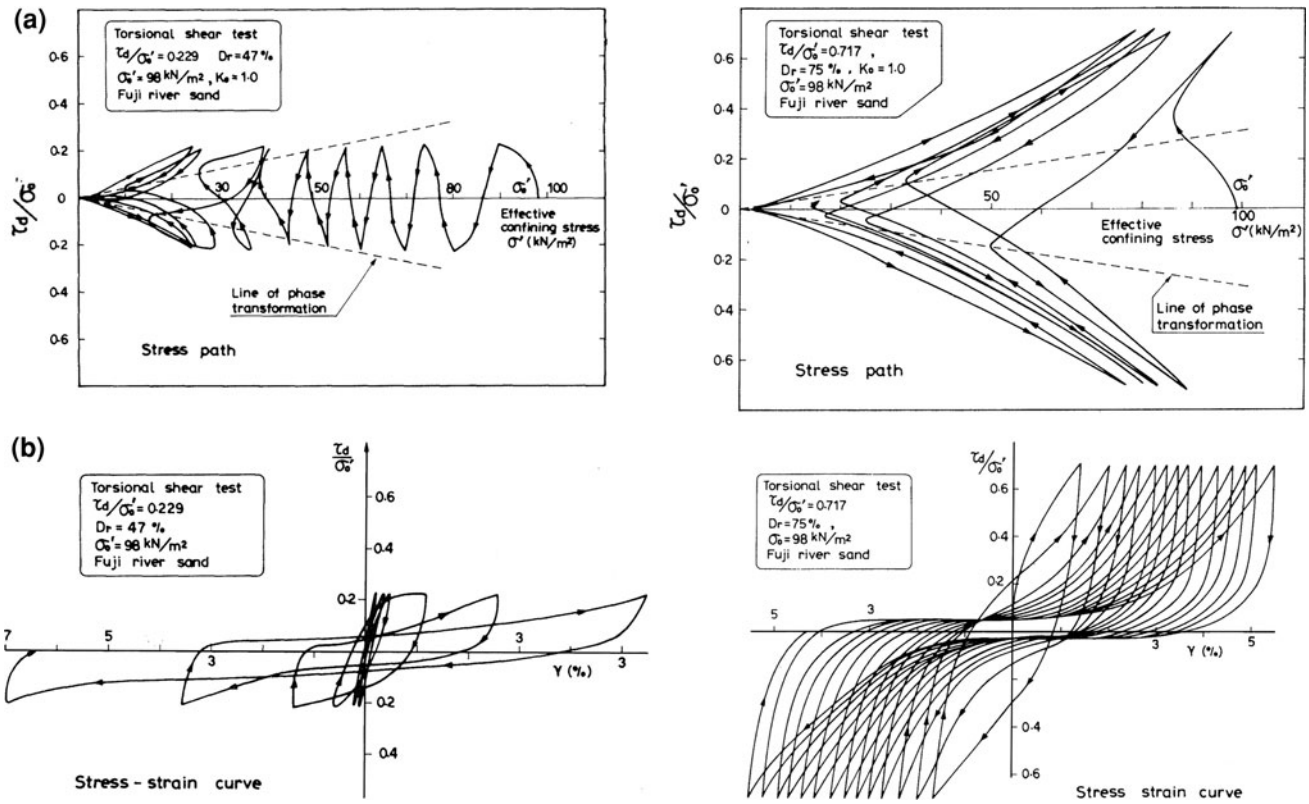

Fig. 7 Cyclic torsional tests on loose and dense sands (after Ishihara and Li [15] and Ishihara [16])

Excess Pore Pressures

Comparing Figs. 11 and 12, it can be seen that both soil models experience excess pore water pressures of about 140 kPa, equivalent to the total vertical stress at the depth of the instrument. This $\sigma_v = u_{\text{excess}}$ line is plotted in these figures as a dashed line to indicate soil liquefaction following the definition given by Eq. 1. The main difference in the excess pore pressure traces is that for the case of dense sand shown in Fig. 12, the dilation is stronger, manifested as larger amplitude suction cycles being superposed on the excess pore pressure generated. It may also be noted that during these large suction cycles, the excess pore pressure temporarily exceeds the dashed line suggesting that the excess pore pressures are greater than the total stress for those brief moments. This is only possible if vertical equilibrium is not maintained at those moments, i.e. the soil body has to accelerate vertically upwards.

Further it can be seen in Figs. 11 and 12 that the soil starts to reconsolidate after the end of earthquake as the excess pore pressures slowly start to dissipate. The rates of excess pore pressure dissipation are very similar for both loose and dense sands. Brennan and Madabhushi [4] showed that the co-efficient of consolidation can be calculated for the liquefied soil in this period.

Soil Settlements

In Figs. 11 and 12, the settlements suffered by loose and dense sands are presented. It can be seen that the loose sand suffers a total settlement of about 0.37 m while that for dense sand is less than half of this value being about 0.18 m. This is to be expected, as the dense sand suffers much smaller volumetric strains compared to loose sands even in the triaxial tests (see Fig. 7).

In Figs. 11 and 12 it can also be seen that the rate of settlement is steepest in the co-seismic period, reducing to a much smaller value in the post-seismic period. This is true for both loose and dense sands. This observation is important, as settlement during the co-seismic period is only possible if the liquefied soil is not behaving in an undrained fashion. As these are level sand beds with no driving shear stresses induced by foundations etc., the rapid co-seismic settlements imply that some drainage of pore fluid is occurring to allow for the soil settlements. Thus the hypothesis of liquefaction being a partially drained event based on the soil stress state reaching the fracture line, as discussed in the previous section, is at least a plausible explanation for these rapid rates of settlement. A corollary to this observation is that thorough introspection is needed in using undrained cyclic triaxial tests to investigate the liquefaction behaviour of saturated sands.

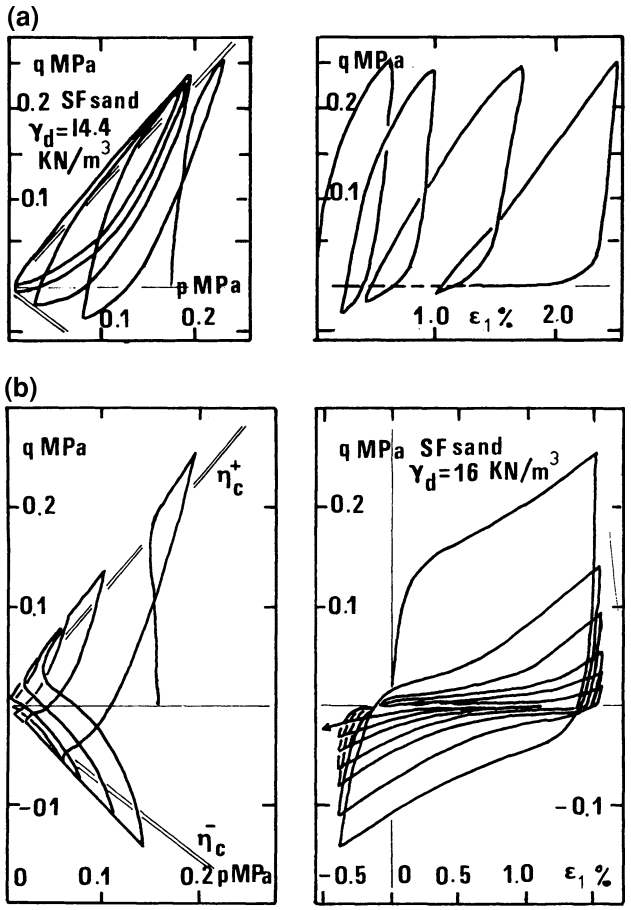

Fig. 8 Cyclic triaxial tests on **a** loose and **b** dense sands (after Luong and Sidaner [20])

Further, if one considers the soil stress state immediately after the end of the earthquake loading in Figs. 11 and 12, the excess pore pressures in the soil at this stage are still high and closely match the total stress. However, the rate of settlement changes abruptly after the end of the earthquake loading. Applying the definition given in Eq. 1, both soils are 'liquefied' at this stage. There must be a change in the behaviour of the soil to cause a change in the settlement rate. This aspect is further considered in developing a micro-mechanical model for soil liquefaction.

Liquefaction Effects on Shallow Foundations

A soil element below the foundations of a structure or in sloping ground will be subjected to static shear stress. In the presence of this static shear stress, the behaviour of a saturated soil element subjected to cyclic shear stresses from an earthquake will be different. In Fig. 9, Arulmoli et al. [2] based on their triaxial tests on Nevada sand show that the stress strain loops of a soil element become asymmetric when an initial shear stress is present.

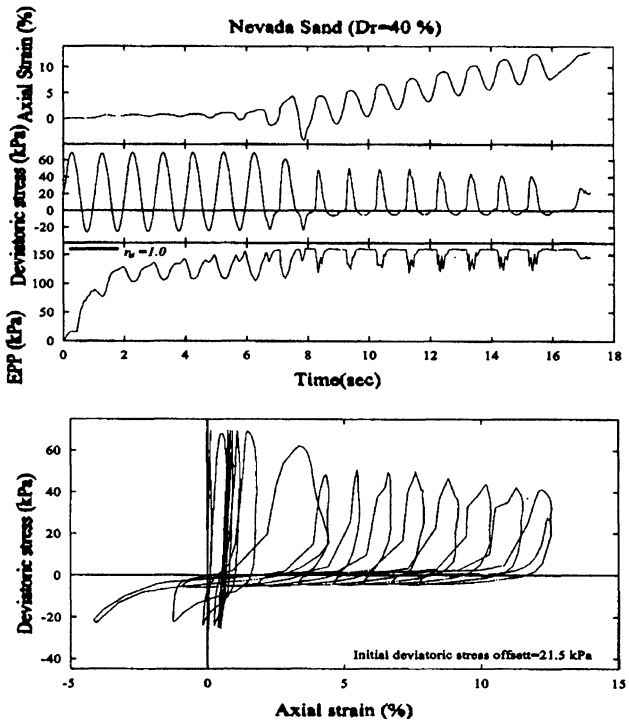

Fig. 9 Stress controlled triaxial tests on loose Nevada sand with initial static shear stress (after Arulmoli et al [2])

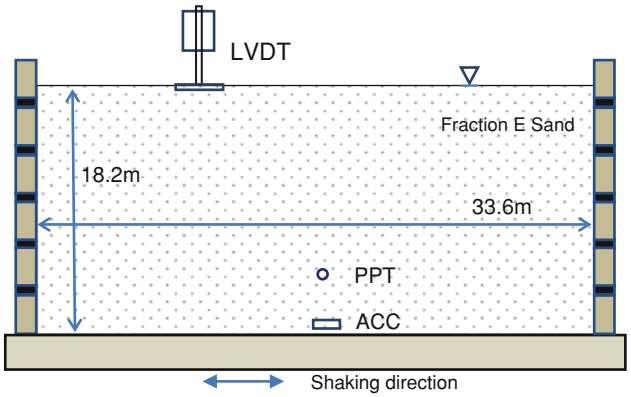

Fig. 10 Cross-sectional view of the centrifuge model in an ESB model container

Liquefaction underneath shallow foundations was investigated by Mitrani and Madabhushi [21] as part of the NEMISREF project. In this study the main focus was on settlements suffered by buildings with shallow foundations located on liquefiable soils and methods that can be used to reduce such settlements. In Fig. 13 the cross-section of centrifuge model BM-1 tested in this study is presented. Hostun sand was used in this study, with properties similar to those of the Fraction E sand used earlier. The sand was placed at a relative density of 46 % and was fully saturated with the water table held at the soil surface. The structure was a single degree of freedom sway frame structure on a

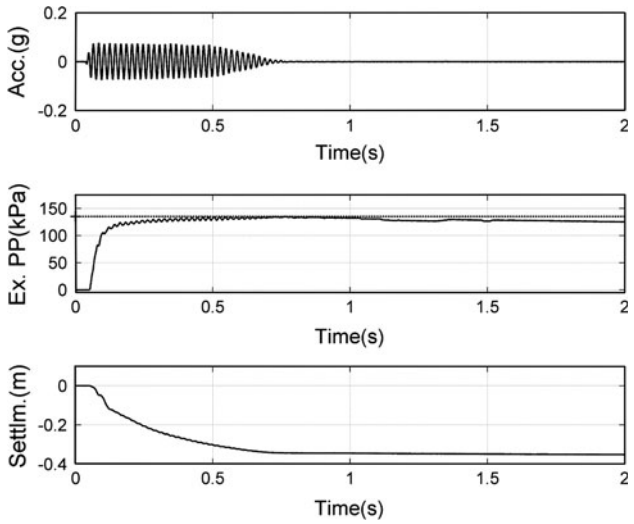

Fig. 11 Results from the centrifuge test on a soil model with a RD of 50 %

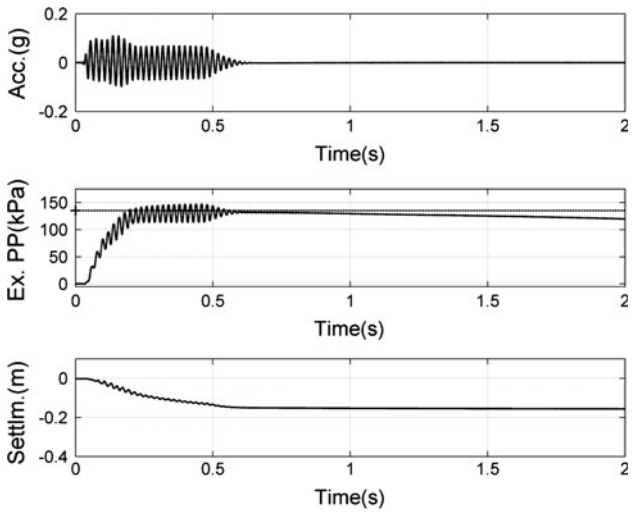

Fig. 12 Results from the centrifuge test on a soil model with a RD of 80 %

shallow foundation that exerted a bearing pressure of 50 kPa on the soil. Although the centrifuge model was heavily instrumented, only the settlements of the structure and the free-field soil surface will be presented here. Cemented zones were also created underneath the shallow foundation in a separate centrifuge test, CZ1F, to investigate the reduction in liquefaction induced settlements. Further details of this study can be found in Mitrani and Madabhushi [21].

In Fig. 14 the settlements of the structure and the soil surface in three successive earthquakes are presented. The amplitude of the input acceleration was increased in successive earthquakes. Earthquake 1 was subjected to an input acceleration of $0.05 \times g$ at the base of the model, while earthquakes 2 and 3 were subjected to 0.2 and

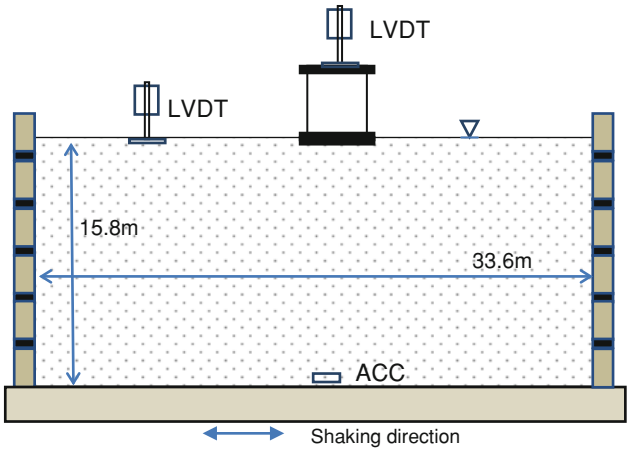

Fig. 13 Cross-section of centrifuge model BM-1 of a shallow foundation (after Mitrani and Madabhushi [21])

$0.25 \times g$, respectively. The vertical dashed line demarcates the end of earthquake loading in Fig. 14. In this figure it can be seen that the soil and structural settlements were quite small in earthquake 1 as the soil did not liquefy. However, in earthquakes 2 and 3 the soil did suffer full liquefaction (as in the case of level sand beds discussed earlier) and the structure and soil surface suffer settlements in these earthquakes. It can be seen in Fig. 14 that in earthquake 2, the free-field soil surface settled by about 0.18 m while the structure settled by 0.35 m. Similar settlements were also recorded in earthquake 3 when the soil was re-liquefied.

As with the level sand bed centrifuge tests, the rate of settlement is much higher during the co-seismic period than in the post-seismic period. This is true for both the structural settlements and the free-field soil surface settlements. Again such rapid rates of settlements are only possible if some amount of drainage of the pore fluid can take place during the earthquake loading. Thus soil liquefaction cannot be treated as an 'undrained event'.

Unlike the level sand bed case, the shallow foundations can suffer settlements during the earthquake due to the soil below the foundation suffering monotonic shear strains. These can give rise to settlements by virtue of liquefied soil displacing from below the foundation through a bearing capacity failure mechanism. Such settlements will be superposed onto the settlement of the ground due to rapid drainage of pore fluid as cracks and fissures open up in soil that has generated excess pore pressures and reached the fracture line. The structural settlements recorded in the centrifuge tests are a combined measure of both these effects.

Focussing on the rates of settlements in earthquakes 2 and 3, the rapid settlement of the structure does indicate that the liquefied soil is able to both drain and undergo shear deformations more rapidly during earthquake loading

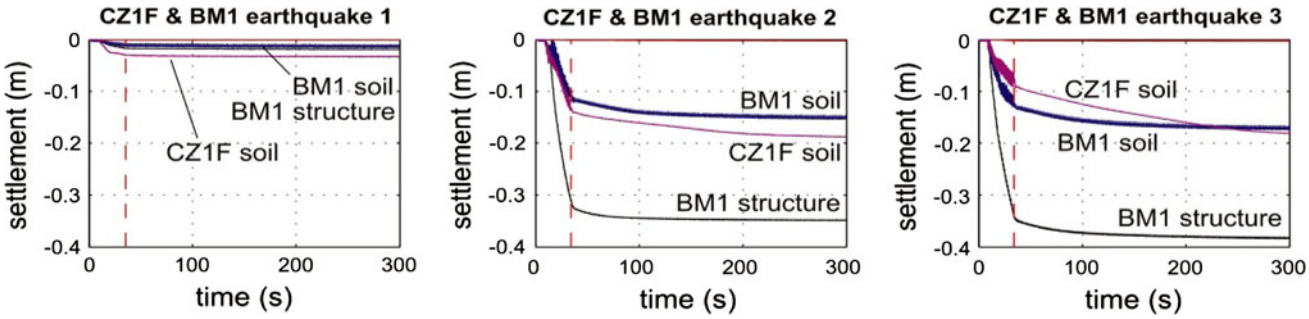

Fig. 14 Settlement of a shallow foundation (after Mitrani and Madabhushi [21])

than after the end of the earthquake. There is a distinct change in the rate of settlement in the co-seismic and post-seismic periods.

Permeability of Soil in Near Liquefied States

Based on the results presented for level sand bed and shallow foundation centrifuge tests, it is clear that the liquefied soil is able to drain more rapidly during earthquake loading than otherwise. This is only possible if the permeability of the liquefied soil can increase rapidly when the soil reaches a near zero effective stress state. Haigh et al. [12] conducted permeability tests in a soil column with an upward hydraulic gradient. The upward hydraulic gradient was adjusted so that the effective vertical stress in the soil could be varied between 0 and 1 kPa. They investigated different types of soil including Fraction E and Hostun sands.

The changes in permeability with decreasing effective vertical stress are presented in Fig. 15. In this figure the permeability is normalised by the value measured at an effective stress of 1 kPa and plotted as the ordinate. It can be seen that the permeability of sands starts to increase rapidly when the effective stress drops to below 0.1 kPa. A power law of the form shown in Eq. 2 can be fitted to the permeability data for different sands.

$$k = k_o\left(\sigma'_v\right)^{\alpha} \tag{2}$$

The variation in permeability is most significant for finer sands such as Fraction E and less obvious in coarser sands such as Fraction D.

Data presented in Fig. 15 confirms that the permeability does in fact change rapidly at very low effective stresses of less 0.1 kPa. In other words if the soil stress approaches near zero values, the permeability of the soil can increase rapidly allowing for rapid pore fluid migration. The condition of the soil at those very low effective stresses is far from being 'undrained'.

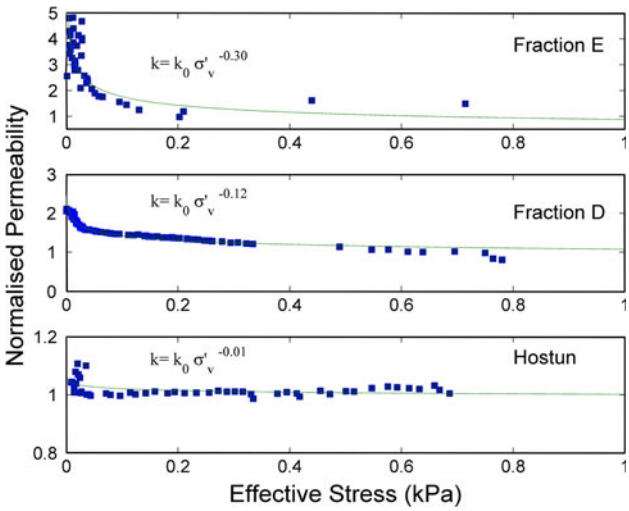

Fig. 15 Change in permeability at very low effective stresses (after Haigh et al [12])

A Micro-Mechanical View of Liquefaction

Historically, soil liquefaction due to earthquake loading was thought to be a rapid event and that consequently the soil would behave in an undrained fashion. As a result, most research was predicated on observations from undrained soil element tests such as cyclic triaxial tests or cyclic torsional tests. In addition the definition of liquefaction was developed based on the concept of excess pore pressure generated in soil matching the initial total stress leading to a near zero effective stress. In this paper it has been established that there is significant evidence that soil liquefaction is not an undrained event. Rapid drainage from the soil does occur during the earthquake loading. Further it has been shown that the settlement behaviour of liquefied soil strata changes following the end of earthquake loading although the excess pore pressures in the soil are still high enough to maintain soil in a 'liquefied' state. These observations call for a change in the established view of soil liquefaction. To address this issue the following hypothesis is offered.

Using the Critical State concept of liquefaction presented in Fig. 4, it can be argued that the dynamic loading of loose, granular soils causes generation of excess pore water pressures that will take the stress path of the soil towards the fracture line. Once the stress path reaches the fracture line, clastic breakage of continuum will occur allowing the formation of cracks and fissures. This will lead to an increase in the permeability of the soil, particularly when the effective stresses are less than 0.1 kPa. This increased permeability will allow the liquefied soil to conduct water rapidly, thereby making the soil settle rapidly and making the liquefied soil behave in a partially drained fashion.

It appears that the loss of effective stress alone is not a sufficient condition for this partially drained behaviour to occur leading to rapid settlements, continued earthquake loading is also required to maintain the soil particles in a near suspended state with very low contact stresses between particles. As soon as earthquake loading stops, the particles begin to come together increasing effective stresses and the permeability rapidly falls back to its normal value. This decreases the rate of settlement in the post-seismic period, as demonstrated by the centrifuge test data on level sand beds and for shallow foundations.

The above hypothesis requires soil liquefaction to be viewed both as a partially drained event and as a dynamic event. Drainage conditions become very important when investigating boundary value problems. The hypothesis will have important implications to numerical modellers using FE analyses. Constitutive modellers need to include changes in permeability at very low effective stresses in their formulations. Further, they need to validate their models not against undrained triaxial data but by using centrifuge test data for well-established boundary value problems.

Conclusions

This paper investigates the current understanding of earthquake-induced soil liquefaction phenomena. The basic definition of liquefaction based on an effective stress concept is presented. Historical studies of liquefaction based on cyclic triaxial tests and the evolution of the Critical State framework for liquefaction that aims to explain the behaviour of saturated granular media subjected to cyclic loading is presented. The evolution of site tests such as SPT and CPT to establish liquefaction potential of sites is explained. Much of this understanding relies on undrained triaxial and torsional testing which assumes that liquefied soil behaves in an undrained fashion owing to rapid earthquake loading.

In this paper evidence is presented based on centrifuge tests on level sand beds and on shallow foundations that the settlement rate of the soil surface as well as any structure founded on liquefiable soils can be high during the earthquake loading, changing to a much lower rate after the end of the earthquake. This implies that soil liquefaction is not an undrained event but is in fact partially drained. While experimental data shows an increase in soil permeability at very low effective stresses, the change in settlement rates post-earthquake while the soil is still liquefied implies the importance of the dynamic nature of the loading. Based on these observations a micro-mechanical view of liquefaction is presented that builds on the Critical State framework with the soil stress state approaching the fracture line. A hypothesis is proposed that;

- Liquefied soil behaves in a partially drained fashion and that
- Very low effective stresses and dynamic loading are both necessary conditions that need to be captured for an accurate understanding of soil liquefaction.

References

1. Andrus RD, Stokoe KH (2000) Liquefaction resistance of soils from shear wave velocity. J Geotech Geoenviron Eng, ASCE 126(11):1015–1025
2. Arulmoli K, Muraleetharan KK, Hossain MM, Fruth LS (1992) VELACS laboratory testing program, soil data report, The Earth Technology Corporation Project No: 90–0562. Irvine, California
3. Beaty MH, Byrne P (2007) Liquefaction and deformation analysis using a total stress approach. J Geotech Geoenviron Eng 134(8):1059–1072
4. Brennan AJ, Madabhushi SPG (2011) Measurement of coefficient of consolidation during reconsolidation of liquefied sand. ASTM Geotech Test J 34(2):64–72
5. Casagrande A (1936) Characteristics of cohesionless soils affecting the stability of slopes and earth fills. J Boston Soc Civ Eng 1:257–294
6. Casagrande A (1971) On liquefaction phenomena, reprinted in Geotechnique 21(3):1–21
7. Castro G (1969) Liquefaction of sands. PhD Thesis, Harvard University; reprinted as Hazard Soil Mechanics Series, No. 8, p l–112
8. Coelho PALF, Haigh SK, Madabhushi SPG, O'Brien AS (2007) Post-earthquake behaviour of footings when using densification as a liquefaction resistance measure. Ground Improv J 11(1):45–53
9. Dixon SJ, Burke JW (1973) Liquefaction case history. J Soil Mech Found Eng, ASCE 99:921–937
10. Finn WDL, Yogendrakumar M, Yoshida N, Yoshida H (1986) TARA-3: a program to compute the response of 2-D embankments and soil-structure interaction systems to seismic loading. University of British Columbia, Vancouver
11. Ghosh B, Madabhushi SPG (2007) Centrifuge modelling of seismic soil-structure interaction effects. J Nucl Eng Des 237:887–896

12. Haigh SK, Eadington J, Madabhushi SPG (2012) Permeability and stiffness of sands at very low effective stresses. Geotechnique 62(1):69–75
13. Idriss IM, Boulanger RW (2006) Semi-empirical procedures for evaluating liquefaction potential during earthquakes. J Soil Dynam Earthquake Eng 26:115–130
14. Ishihara K, Tatsuoka F, Yasuda S (1974) Undrained deformation and liquefaction of sand under cyclic stresses. Soil Found 15(1):29–44
15. Ishihara K, Li S (1972) Liquefaction of saturated sand in triaxial torsional shear test. Soil Found 12(2):19–39
16. Ishihara K (1985) Stability of natural deposits during earthquake. In: Proceedings of XI international conference on soil mechanics and geotechnical engineering, San Francisco, vol. 1
17. Ishihara K (1993) Liquefaction and flow failure during earthquakes. Geotechnique 43(3):351–415
18. Kramer SL (1996) Geotechnical earthquake engineering. Prentice Hall Inc., New Jersey. ISBN 013374943-6
19. Luong MP (1980) Stress–strain aspects of cohesionless soils under cyclic and transient loading. In: Proceedings of international symposium on soil under cyclic and transient loading, Swansea, p 315–324
20. Luong MP, Sidaner JF (1981) Undrained behaviour of cohesionless soils under cyclic and transient loading. In: Proceedings of international conference on recent advances in geotechnical earthquake engineering and soil dynamics. St Louis, USA
21. Mitrani H, Madabhushi SPG (2010) Cementation liquefaction remediation for existing building. Ground Improv J 163(G12): 81–94
22. Madabhushi SPG, Haigh SK (2009) Effect of superstructure stiffness on liquefaction-induced failure mechanisms. Int J Geotech Earthquake Eng 1(1):72–88
23. Madabhushi SPG (2008) Future trends in geotechnical earthquake engineering. In: Sitharam TG, Babu GLS (eds) Proceedings of Indian geotechnical conference. Key Note Lecture, Indian Institute of Science, Bangalore, pp 379–389
24. Madabhushi SPG, Thusyanthan I, Lubkowski Z, Pecker A (2008) In: Elghazouli A (ed) Shallow Foundations, Seismic design of buildings to Eurocode 8. Spon Press, London. ISBN 9780415 44762-1
25. Muhunthan B, Schofield AN (2000) Liquefaction and dam failures. Proc GeoDenver, Denver
26. Robertson PK, Wride CE (1998) Evaluating cyclic liquefaction potential using the cone penetration test. Can Geotech J 35(3): 442–459
27. Roscoe KH, Schofield AN, Wroth CP (1958) On the yielding of soils. Geotechnique 8:22–53
28. Schofield AN (1980) Cambridge geotechnical centrifuge operations. Geotechnique 25(4):743–761
29. Schofield AN (1981) Dynamic and earthquake geotechnical centrifuge modelling. In Proceedings of international conference on recent advances in geotechnical earthquake engineering and soil dynamics, St Louis, vol. III, pp 1081–1100
30. Schofield AN, Wroth CP (1968) Critical state soil mechanics. McGraw-Hill, London
31. Seed HB, Lee KL (1966) Liquefaction of saturated sands during cyclic loading. ASCE J Soil Mech Found Eng 92:105–134
32. Seed HB, Lee KL, Idriss IM (1969) Analysis of Sheffield dam failure. ASCE J Soil Mech Found Eng 95:1453–1490
33. Seed HB, Idriss IM (1971) Simplified procedure for evaluating soil liquefaction potential. J Soil Mech Found, ASCE 97(SM9): 1249–1273
34. Seed HB (1979) Soil liquefaction and cyclic mobility evaluation for level ground during earthquakes. ASCE J Geotech Eng 105(2):201–255
35. Tokimatsu K, Seed HB (1987) Evaluation of settlements in sand due to earthquake shaking. J Geotech Eng ASCE 113(8):861–878
36. Zienkiewicz OC, Chan AHC, Pastor M, Schrefler BA, Shiomi T (1999) Computational geomechanics. Wiley, USA. ISBN 9780 471982852